Title
HYDROCARBON HEAT TRANSFER COEFFICIENTS: PRELIMINARY ISOBUTANE RESULTS

Authors
Tleimat, B.W.
Laird, A.D.K.
Rie, H.
et al.

Publication Date
1979-02-01

DISCLAIMER

LBL-8645

HYDROCARBON HEAT TRANSFER COEFFICIENTS: PRELIMINARY ISOBUTANE RESULTS*

B.W. Tleimat, A.D.K. Laird, H. Rie,
I.C. Hsu, and R.A. Seban

Earth Sciences Division
Lawrence Berkeley Laboratory
University of California, Berkeley, California 94720

February 1979

Abstract

Research designed to obtain baseline heat transfer data on secondary fluid candidates for geothermal cycle systems is described. The apparatus was designed to provide baseline data under clean conditions to determine inside and outside heat transfer film coefficient, respectively, for heating and condensation of secondary fluids being considered for binary systems. The secondary fluid loop simulates the binary cycle with steam, instead of geothermal fluid, as the heating fluid and a throttling valve instead of the turbine.

In this report, results on film coefficient for condensing the isobutane on the outside of a tube at various pressures and condensate loading, as well as preliminary results on film coefficient for heating the isobutane inside a tube at 4.14 MPa (600 psia) and various flow rates, are presented. The isobutane was heated in a horizontal, type 316 stainless steel, instrumented tube by steam condensing on the outside. In the condenser, the isobutane was condensed on the outside of a horizontal tube, identical to that in the heater, by cooling water inside the tube. Each instrumented tube was fitted with a total of fifteen thermocouples imbedded in the wall of the tube at five stations located equally along the length of the tube. The inside and outside wall temperature of the tube at each of the five stations was calculated from the location of the imbedded thermocouples and their temperatures. The heat rate to the isobutane in the heater was determined by measuring the rate of condensing steam on the outside of the tube under each of four sections by means of specially designed vapor-traced meters. The heat rate released by the condensing isobutane was also determined by measuring the rate of isobutane condensing on the outside of the tube with meters similar to those in the heater.

---

*Prepared for the U.S. Department of Energy, Division of Geothermal Energy, under Contract No. W-7405-ENG-48.

The temperature of the isobutane inside the heater tube was measured by a traveling platinum resistance thermometer equipped with a mixing head at its tip and the temperature of the condensing isobutane in the condenser chest was measured by a platinum resistance thermometer.

Film coefficients for the heating of isobutane in the range of 540-2100 W/m^2C (95-370 Btu/hr ft^2 ^oF) were obtained for Reynolds number between 2 x 10^4 to 2 x 10^5. Film coefficients for the condensation of isobutane in the range of 568-2270 W/m^2C (100-400 Btu/hr ft^2 ^oF) were obtained at temperatures ranging between 49-99^oC (120-210^oF) and condenser loading ranging between 20-1030 Kg/hr m^2 (4-210 lbs/hr ft^2).

CONTENTS

HYDROCARBON HEAT TRANSFER COEFFICIENTS: PRELIMINARY ISOBUTANE RESULTS

Introduction

Assessments of the potential of geothermal energy resources have pointed to hot brines as a viable source of large amounts of geothermal power in the next two or three decades. Power plant feasibility studies (Roberts, 1976) and recent exploratory drilling (Wollenberg, et al., 1975) tend to confirm this opinion, and show further that low-salinity intermediate temperature (150-230°C) brines are the most plentiful.

To take full advantage of this source of energy, the binary cycle has been proposed, particularly with brines in the lower part of the temperature range or with brines at high salinities and/or with brines that have noncondensable noxious gases. In this system, geothermal brine is used to heat another or secondary fluid used as the working fluid of a turbo-generator power cycle much as in an ordinary steam power plant. Depending on the temperature range and other conditions, the secondary fluid may be water, ammonia, refrigerants, isobutane, other fluids, or appropriate mixtures of fluids. Although isobutane has received the most attention for use in the intermediate temperature range, mixtures of isobutane and isopentane, Freons 22 and 113, and ammonia are being considered.

Heat transfer equipment, principally to heat and condense the secondary fluid, accounts for approximately half the capital cost of the binary cycle geothermal plant. That this cost is significant was shown by the cost estimate for a 10 MW experimental power generation facility, prepared for the Lawrence Berkeley Laboratory by Rogers Engineering Company, Inc. and Benham-Blair and Affiliates (1974). The estimated installed cost of the plant, excluding brine production and injection wells, was expected to be $12 million, of which the heat transfer equipment accounted for $6 million. On the same basis, the heat transfer equipment alone for a 50 MW plant would cost about $30 million. In such cases, an inexact estimate of the heat transfer coefficients can have serious effects. If the coefficients used in the design are too high, the plant may fail to meet its performance guarantee. If much too low, the plant will be overdesigned and wasteful.

In specifying heat transfer equipment for a process, the designer is usually armed with well tested information on the performance of similar equipment under similar or identical conditions. In an unusual application, such as specifying heat transfer equipment in a geothermal binary cycle plant using isobutane as the working fluid, the engineer is forced to search the literature for design information. In the absence of data specifically applicable to the design at hand, designers usually refer to the heat transfer coefficient prediction methods embodied in the correlation equations of Dittus and Boelter, of Colburn, and of Sieder and Tate found in standard works. These general correlations are based on fluid transport properties and give the mean, or

most probable value of a large amount of reliable experimental data. Unfortunately, because of the large influence sometimes exerted on heat transfer by minor and frequently unrecognized variations in conditions, a designer can only be reasonably sure that the performance of an individual heat exchanger will be within plus or minus 35 percent of the mean. Consequently, to assure fulfillment of a performance guarantee on a design embodying a minor innovation, the designer would select a heat transfer coefficient value at the lower limit, that is, 35 percent less than the mean. It must be noted here that the correlation equations for the prediction of the heat transfer coefficients need accurate and reliable data on the transport properties of the fluid at the operating conditions. Lack of data at these conditions makes the designer's task difficult at best. This lack of data is especially true for designs where the working fluid is in the supercritical region. This is important because computer studies, LBL's GEOTHM, for example (Green and Pines, 1975), indicate that heating of the secondary fluid in the supercritical region results in high cycle efficiency. Consequently, the most effective and reliable method for specifying the equipment is to determine experimentally the value of the heat transfer coefficient at the proposed operating conditions.

The Binary Fluid Experiment (BFE) was designed to provide experimental data to determine heat transfer coefficients of the various candidate working fluids. It will establish baseline data on film coefficients for several light hydrocarbons starting with isobutane, mixtures of light hydrocarbons, refrigerants and ammonia. Data will be gathered from the BFE for the ranges of heating and condensing temperature and pressures that would be expected in geothermal power plant applications.

Experimental Approach

Figures 1 and 2 show the schematic flow diagram and the corresponding pressure enthalpy diagram for an ideal geothermal binary cycle plant in its simplest form. The saturated liquid secondary fluid leaves the condenser at state point 1 where it is pressurized to state point 2 by the condensate pump and heated by the geothermal brine in the heater to state point 3. There it expands isentropically to state point 4 through the turbine where part of its available energy is extracted as mechanical energy. In the condenser, the fluid is cooled and condensed to state point 1 by rejecting its heat to the cooling water.

In transferring heat from the geothermal brine to the secondary fluid in the heater, the overall heat transfer coefficient, U, is given by

$$\frac{1}{U} = R_f + \frac{1}{h_f} + \frac{\ell_m}{k_m} + \frac{1}{h_b} + R_b \qquad (1)$$

where

R_f = fouling resistance on working fluid side;

h_f = film coefficient on working fluid side;

ℓ_m = thickness of heat transfer surface;

k_m = thermal conductivity of heat transfer surface;

h_b = film coefficient on geothermal brine side; and

R_b = fouling resistance on brine side.

A similar relation holds for the condensing working fluid and the cooling water in the condenser.

This experiment has been designed specifically to obtain data to determine the film coefficient and fouling resistance, if any, of the secondary fluid during heating and condensation. Figure 3 is a schematic flow diagram of the BFE. The experimental equipment consists of a stainless steel loop simulating a binary system with steam instead of brine as the heating fluid and a throttling valve instead of the turbine. The pressurized secondary fluid is heated inside a single instrumented tube with steam condensing on the outside of the tube. After heating, the secondary fluid expands through the throttling valve and is introduced into a direct contact desuperheater or a surface desuperheater by means of two three-way valves. After desuperheating, the vapor enters the condenser, condenses on the outside of a single instrumented tube identical to that in the heater but containing cooling water inside. The condensed secondary fluid is collected in the secondary fluid hotwell and enters the booster pump where it is slightly pressurized before entering the high pressure pump. During operating with the direct contact desuperheater, the two three-way valves are positioned so that the secondary fluid, after expansion through the throttling valve, enters the direct contact desuperheater. Also during this mode of operation, a portion of the condensed secondary fluid is diverted to the direct contact desuperheater and the excess is returned to the suction side of the booster pump.

The instrumented tubes in each of the heater and condenser were made from a 31.8 mm (1.25 in.) O.D. and 19.1 mm (0.75 in.) I.D.-type 316 stainless steel tube that was cut into two pieces, about 2.7 m (106 in.) long, and honed to an inside diameter of 19.2 mm (0.756 in.). In order to obtain uniform wall thickness, the two pieces were machined to an outside diameter of 30.2 mm (1.189 in.). The concentricity was then checked by ultrasonic measurement of the tube wall thickness at 101.6 mm (4.0 in.) intervals along the axis. At each location, the wall thickness was measured at four points 90° apart. These measurements were later used to indicate the precise locations of thermocouples imbedded in the wall of each tube.

In order to evaluate the film coefficient and the fouling resistance of the secondary fluid, it is necessary to obtain data to determine

the film coefficient and its variation with time so that fouling resistance, if it exists, can be calculated. The local film coefficient, h_f, is defined as the ratio of the heat flux, q, through the heat transfer surface to the difference between the wall temperature, t_w, and the secondary fluid bulk temperature, t_{fb}, and is given by

$$h_f = \frac{q}{t_w - t_{fb}} \tag{2}$$

The heat flux, q, was determined by measuring the time required to collect a given amount of steam condensate per unit area of tube wall. The wall temperature was determined by imbedding thermocouples in the wall of the tube, as shown in Fig. 4. The bulk temperature of the fluid inside the heater tube was measured by a traveling probe which consisted of a 6.35 mm (0.25 in.) dia. x 2540 mm (100 in.) long stainless steel sheathed platinum resistance thermometer equipped with a mixing head at its tip. Mechanisms and seals were provided to move and locate the probe precisely inside the tube and prevent fluid leakage. In order to maximize the information output from the experiment, a total of fifteen thermocouples were imbedded in the tube at five stations 609.6 mm (24 in.) apart with three thermocouples located at each station, as shown in Fig. 4. By determining the radial location of each of the thermocouples at each station and the temperature at each location, one can determine the inside and outside surface temperature of the tube at this station regardless of the type of material of construction of the tube. Thus, by determining the heat rate input to the secondary fluid between the stations, and measuring the temperature of the vapor outside the tube and the bulk temperature of the fluid inside the tube at each of the stations, it is possible to calculate the average inside and outside film coefficients of the four sections. Also, by calculating the heat rate in each section and measuring the pressure and the bulk temperature of the working fluid at these stations, it may be possible to determine the properties of the fluid at each of the five stations.

The rate of heat input to the secondary fluid in the heater and the rate of heat released by the condensing secondary fluid vapor in the condenser was determined by measuring the rate of condensing vapor on the outside of the tubes at the four sections. This was done by placing a four-section pan under the tube with the five ends of the sections located just underneath the five thermocouple stations. Figure 5 shows a cross section of the heater. It shows the external shell, the instrumented tube with the thermocouples at 45° from the vertical plane, the condensate pan and a hood placed above the tube to prevent any condensate forming on the inside surface of the shell from dripping into the pan. The condensate formed on the outside of the tube dripped into the separate sections of the pan and drained into four specially designed vapor-traced condensate flow meters. The meter had a timer to measure the time required to fill a calibrated volume. The timer was operated by photocells to detect the rising condensate surface between two predetermined levels in the meter.

The temperature of the condensing vapor outside the tube in each of the heaters and the condenser was measured by means of a calibrated platinum resistance thermometer (RTD) and three calibrated type K thermocouples located in the vapor space. The RTD was located at the opposite end from the vapor inlet, while one thermocouple was located at the vapor inlet, the second half-way along the length of the shell, and the third close to the RTD. These three thermocouples were used to check the reading of the RTD and also to indicate the presence of superheat in the vapor. The pressure in the vapor space was measured by means of calibrated pressure transducers. This pressure measurement was used as a check on the saturated temperature of the vapor and also to detect the presence of noncondensable gases in the vapor space.

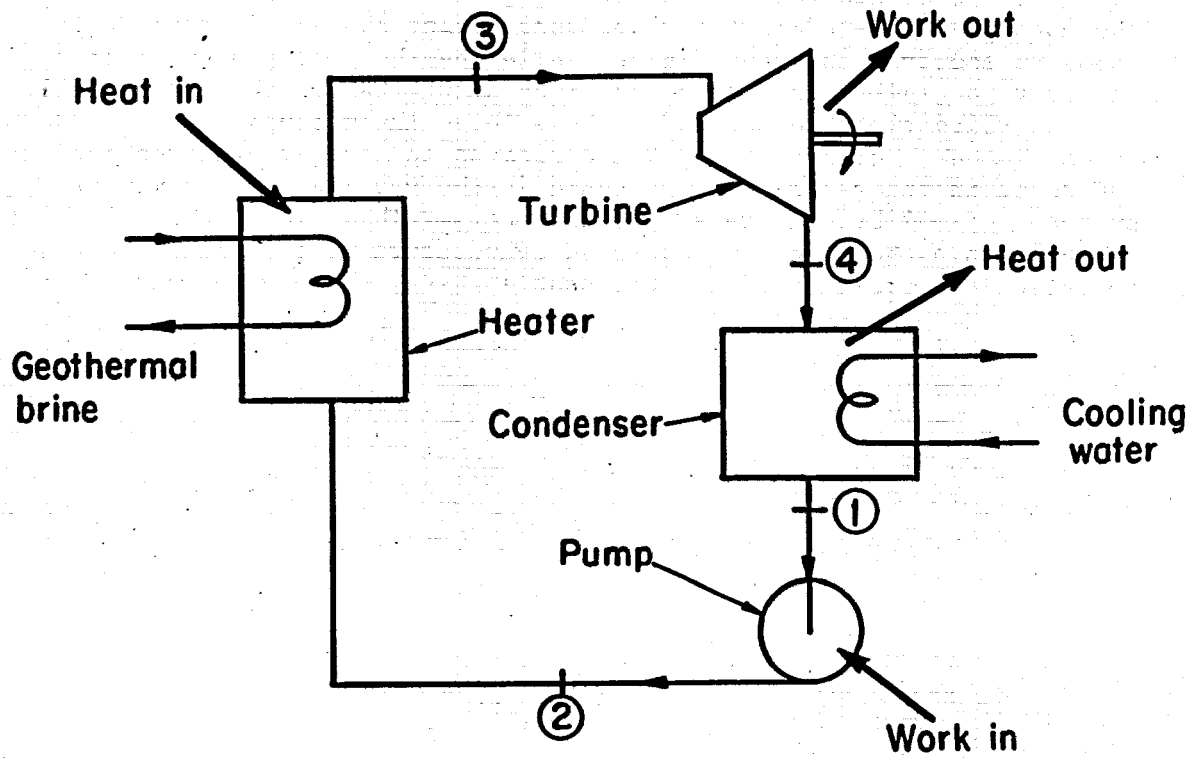

Fig. 1. Simple geothermal binary cycle - Schematic flow diagram.

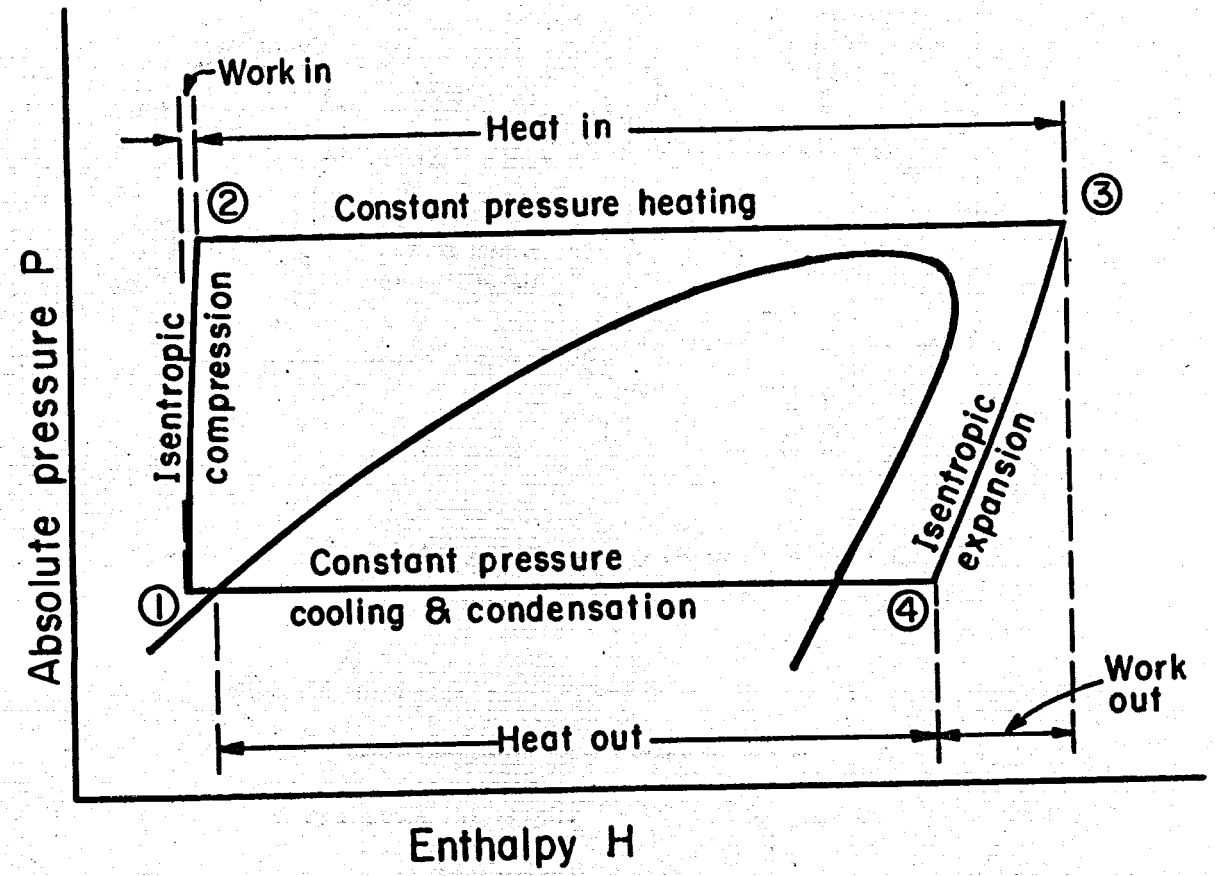

XBL7812-12412

Fig. 2. Pressure-enthalpy diagram for the working fluid corresponding to the cycle in Fig. 1 with heating at supercritical pressure.

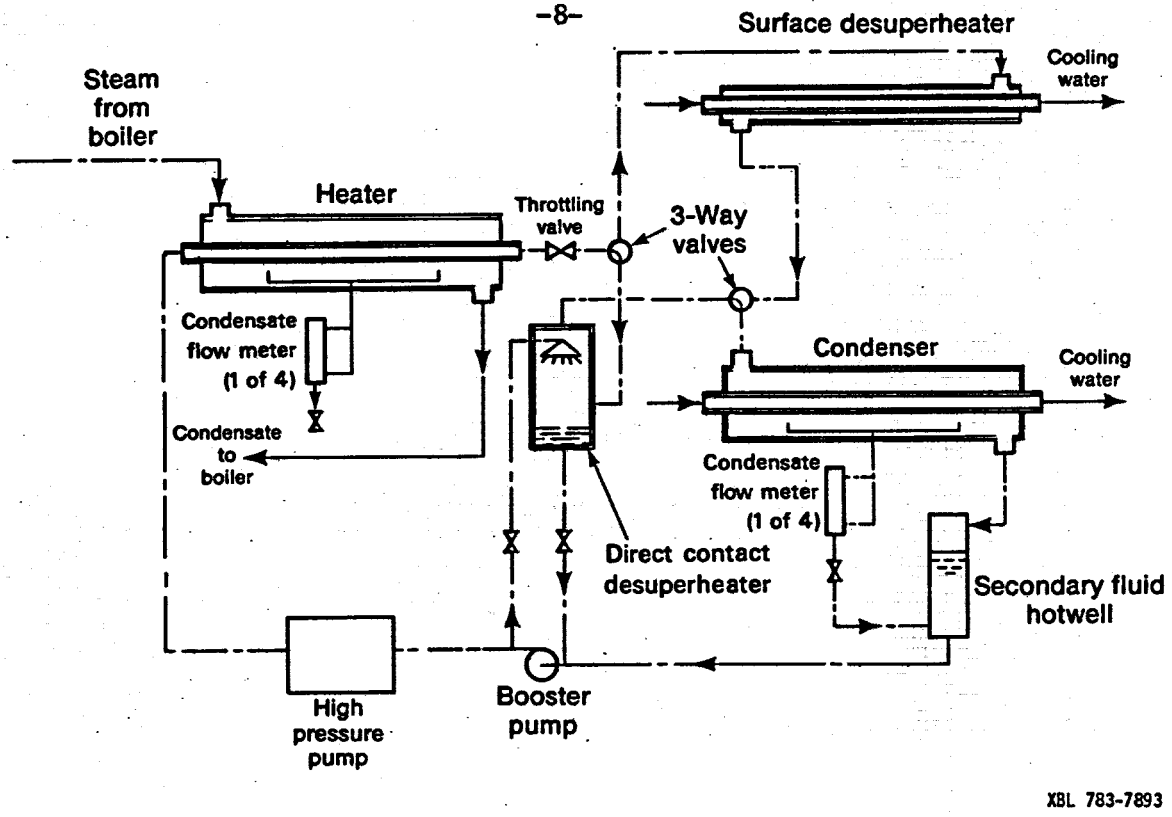

Fig. 3. Schematic flow diagram of the Binary Fluid Experiment.

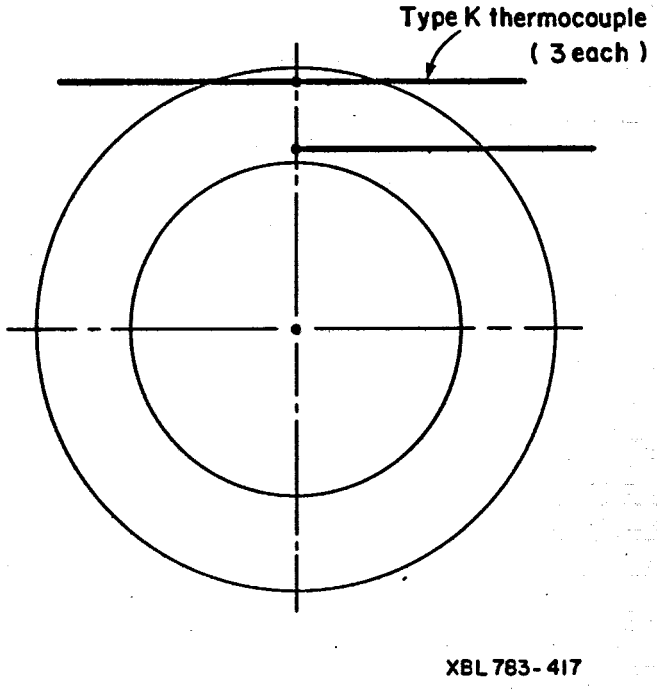

Fig. 4. Tube cross section showing location of thermocouples.

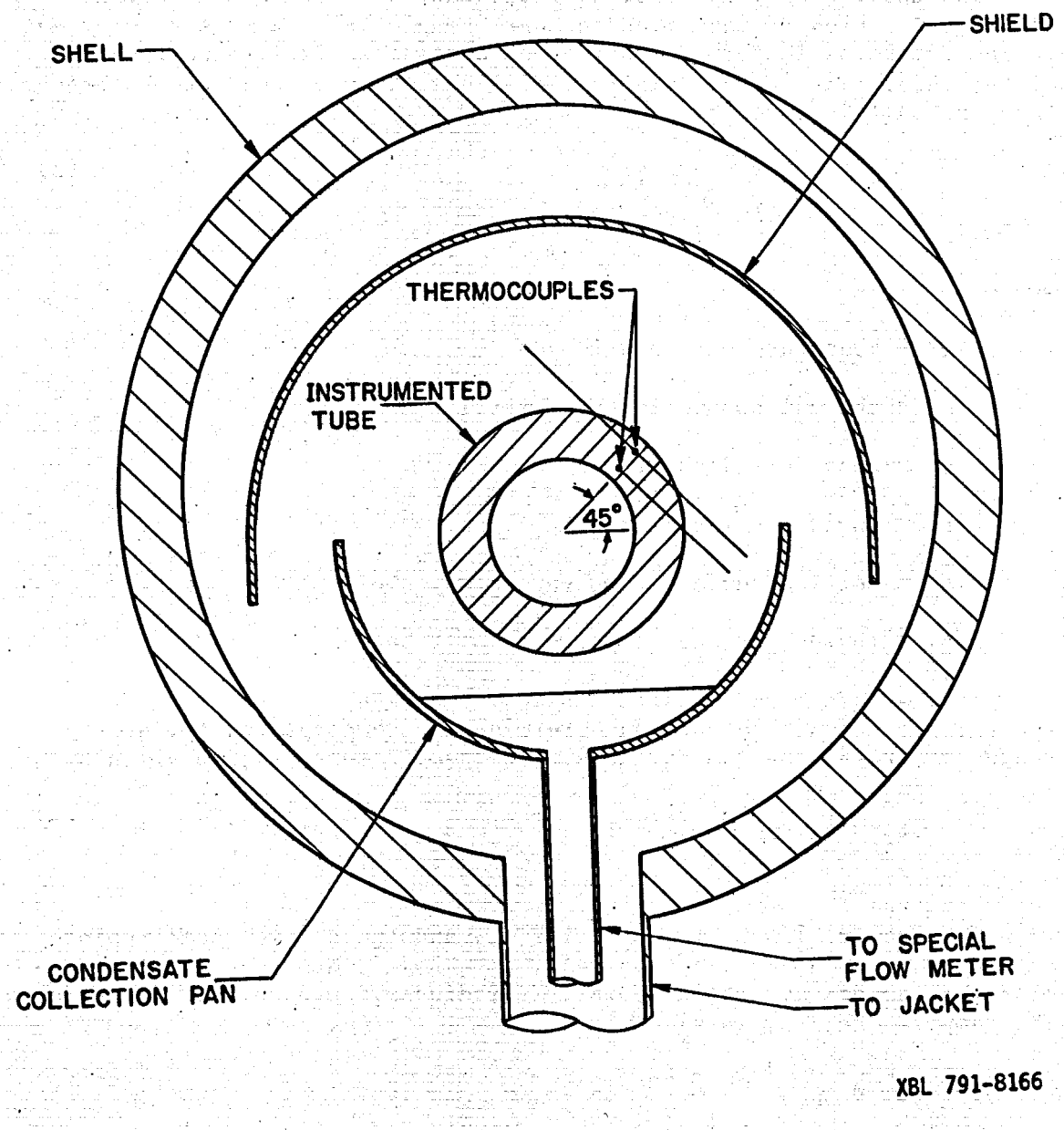

Fig. 5. Heater cross section showing tube, condensate tray, drip shield and outer shell.

Instrumented Tubes

The details of construction of the instrumented tubes together with the location of the imbedded thermocouples are extremely important to the determination of the inside and outside surface temperatures of the tube. The inward uniform radial heat flow by conduction through the tube wall is given by

$$Q = \frac{2\ \pi k_m\ (t_o - t_i)}{\ln \frac{r_o}{r_i}} \tag{3}$$

where

Q = heat rate per unit length

k_m = thermal conductivity of metal

r_o = outside radius of tube

r_i = inside radius of tube

t_o = outside surface temperature of tube

t_i = inside surface temperature of tube

If the inside and outside surface temperature of the tube, t_i and t_o, are known then one can determine the temperature, t_r, at any radius r between the two surfaces. The temperature, t_r, is given by

$$t_r = t_o - \frac{t_o - t_i}{\ln \frac{r_o}{r_i}} \ln \frac{r_o}{r} \tag{4}$$

Conversely, if the temperatures, t_a and t_b, at two radial points at radii, a and b, in the tube wall, are known, then one can also determine the temperature at any point, at radius r, between the two surfaces. The temperature, t_r, is given by

$$t_r = t_b - \frac{t_b - t_a}{\ln \frac{b}{a}} \ln \frac{b}{r} \tag{5}$$

This equation was used to calculate the inside and outside surface temperatures of the instrumented tube in the heater and in the condenser.

Three sheathed and ungrounded thermocouples were imbedded at each of the five stations in the wall of each tube, as shown in Fig. 4. Figure 6 is a photograph showing three thermocouples installed in the tube at one of the stations. One thermocouple was placed close to the inside surface of the tube and two opposing thermocouples were placed

close to the outside surface of the tube. The two opposing thermocouples provide a redundancy in the measurement which may be used to indicate thermocouple malfunctions.

These thermocouples were made from chromel-alumel wire of 0.038 mm (0.0015-in.) dia. enclosed inside a 0.254 mm (0.010-in.) outside diameter type 316 stainless steel sheath. This small size wire as well as the tangential direction of installation were selected to provide the accuracy needed in determining the location of the measuring points in the wall of the test tube, and to minimize the effect on the temperature at the thermocouples of the thickening of the condensate film on the thermocouple sheaths. Due to the small diameter of the sheath and the length of the holes in the tube wall where the sheathed thermocouples were imbedded, the holes were drilled to a diameter of 0.813 mm (0.032-in.) to the required depth. Short pieces of stainless tubes of 0.787 mm (0.031-in.) outside diameter and 0.279 mm (0.011-in.) inside diameter were installed inside the holes in the tube wall and brazed in a hydrogen atmosphere. After brazing, the sheathed thermocouples were inserted inside the small 0.787 mm O.D. tubes and soft soldered in place.

Two important factors were considered during the design of the experiment regarding the orientation of the thermocouples in the instrumented tube. These factors are the effects of buoyancy of the fluid inside the tube on the inside film coefficient, (Adebiyi and Hall, 1976), and the effects of variation of condensation film coefficient of the vapor as a function of angle (Boelter et al., 1946). In order to assess the influence of these two effects, the imbedded thermocouples at three stations, e.g., stations 1, 3 and 5, were located 90° apart from the other two stations, i.e., when the measuring points of the nine thermocouples at stations 1, 3 and 5 are located on one plane along the longitudinal axis of the tube, the other measuring points of the six thermocouples at the other two stations, stations 2 and 4, would be located on a plane along the longitudinal axis of the tube and perpendicular to the other one. Thus, by rotating the test tube, it may be possible to obtain data from which to calculate surface coefficients for the position selected and determine the combined effects of buoyancy and condensation on the inside film coefficient in the heater.

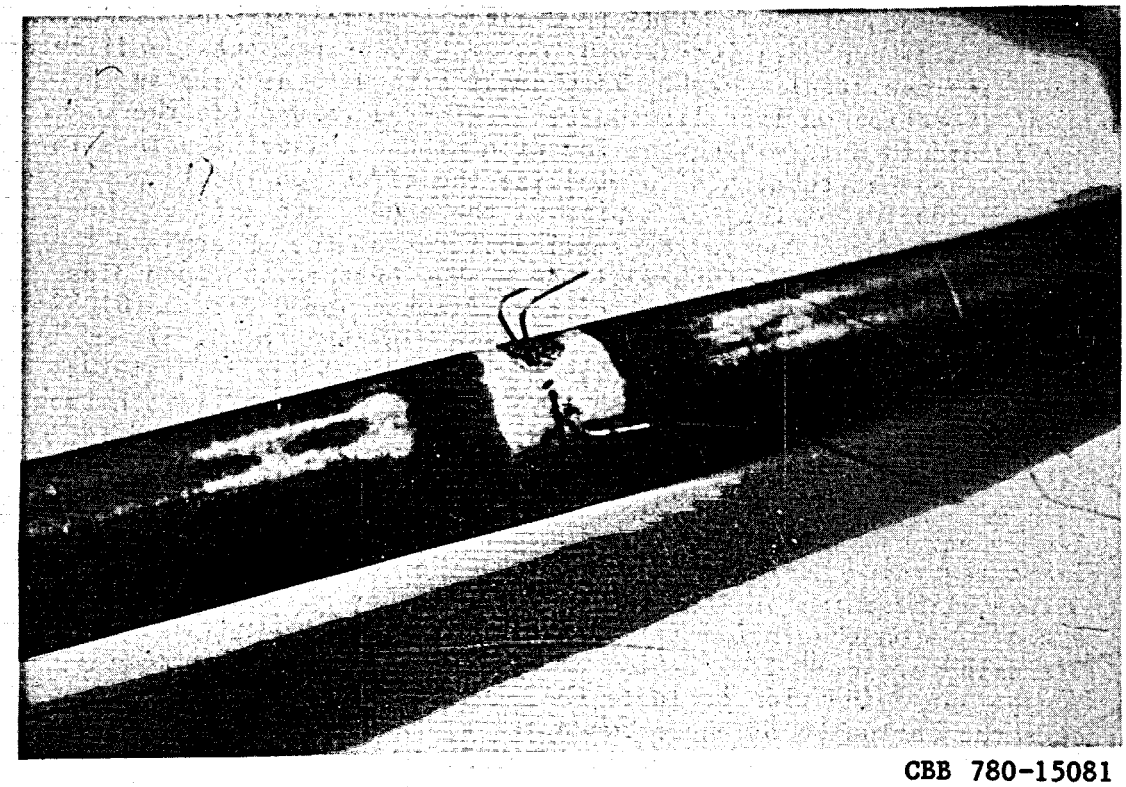

CBB 780-15081

Fig. 6. Instrumented tube with three imbedded thermocouples at one of the five stations.

Experimental Apparatus

Figure 7 is a photograph of part of the apparatus. It shows the heater, the surface desuperheater, the condenser, the special condensate measuring meters, the expansion valve and the high pressure pump. Figure 8 is a detailed flow diagram of the experimental apparatus consisting of the heat supply system, the heat rejection system and the secondary fluid loop. The heat supply system consists of a 4.14 MPa (600 psig) boiler with its associated piping, control valves, condensate hotwell, and condensate return. The heating steam from the boiler is supplied to the preheater through a manual valve and then through a pneumatic control valve to the steam chest in the heater. Condensate dripping from the outside of the instrumented tube and collected in the four-section pan under the tube drains into the specially designed flowmeters, and then drains into the condensate hotwell. Condensate formed on the inside wall of the heater, as well as condensate formed inside the jacket of the flowmeters also drain through a separate tube into the condensate hotwell. The level of the condensate in the hotwell is controlled by a pneumatic control valve which allows the condensate to drain from the hotwell through a cooler, and back to the boiler. Condensate from the preheater drains into the return line downstream from the pneumatic control valve.

The heat rejection system for both the secondary fluid condenser and surface desuperheater is of the feed-and-bleed type. It consists of a loop where the cooling water is circulated inside the tubes at controlled flow rates by means of circulating pumps and throttling valves. Cold water from the municipal water system is introduced at the suction side of each circulating pump and discharged from the loop through a control valve after being heated in the condenser or desuperheater. This allows much finer control of condenser temperature and exit temperature from the desuperheater, as well as permitting the circulating water in the loop to operate at temperatures above 100°C without boiling. The cooling water volumetric flow rate was measured by a calibrated turbine flowmeter and the temperature of the cooling water at the inlet and outlet were measured by means of calibrated platinum resistance thermometers.

The secondary fluid loop consists of a heater, direct contact desuperheater, surface desuperheater, condenser, hotwell, centrifugal-type booster pump, high-pressure diaphragm-type pump, steam preheater, pneumatically-controlled expansion valve, and two pneumatically-operated three-way valves for switching the flow of secondary fluid from one desuperheater to the other. During operation with the direct contact desuperheater, a portion of the secondary fluid from the booster pump is diverted to the direct contact desuperheater to cool the superheated vapor and the excess is returned to the suction side of the booster pump. The volumetric flow rate of secondary fluid in the heater was measured with a turbine flowmeter. The temperature at different points in the loop was measured by means of platinum resistance thermometers and chromel-alumel thermocouples. The pressure of the secondary fluid

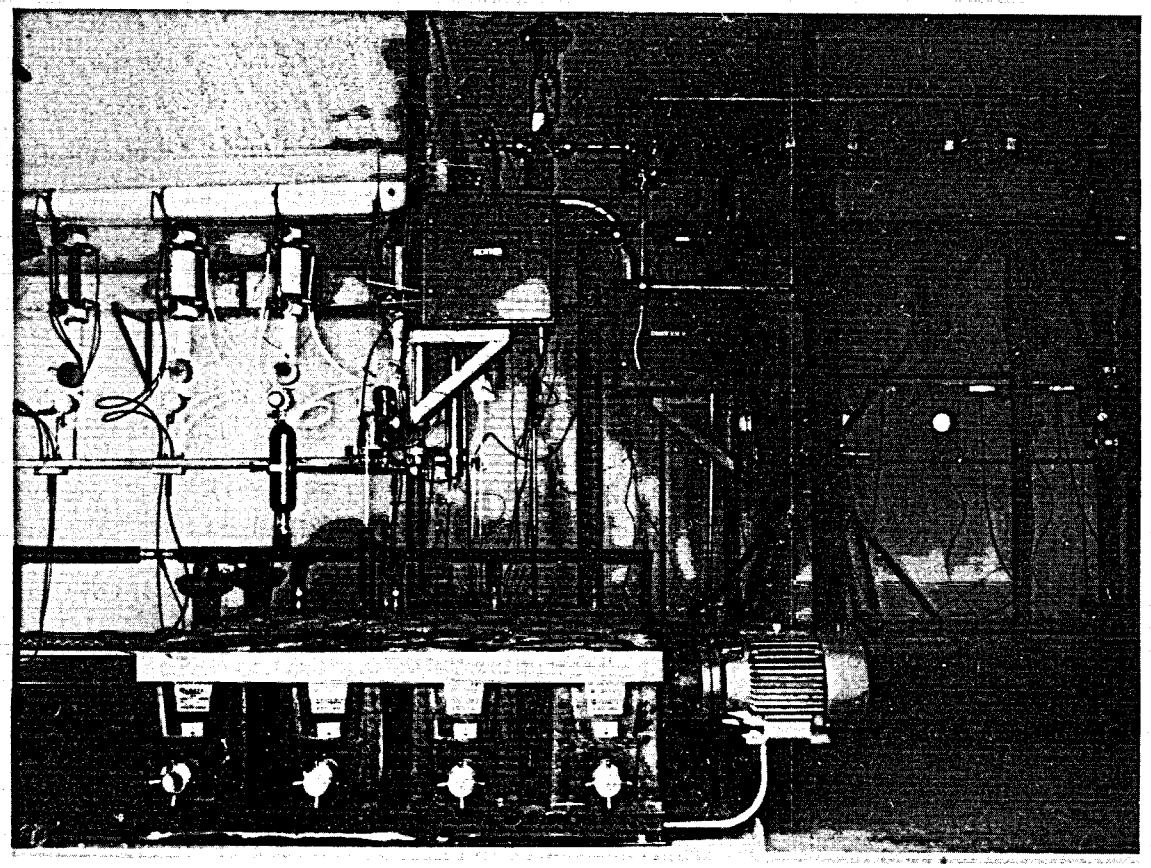

CBB 780-15079

Fig. 7. Binary Fluid Experiment showing the high pressure pump in the foreground, the Isobutane Heater and its special Condensate Flow Meters in the upper left section, the Isobutane Throttling Valve in the mid-section, the Surface Desuperheater and Isobutane Condenser and its special Condensate Flow Meters in the upper right section.

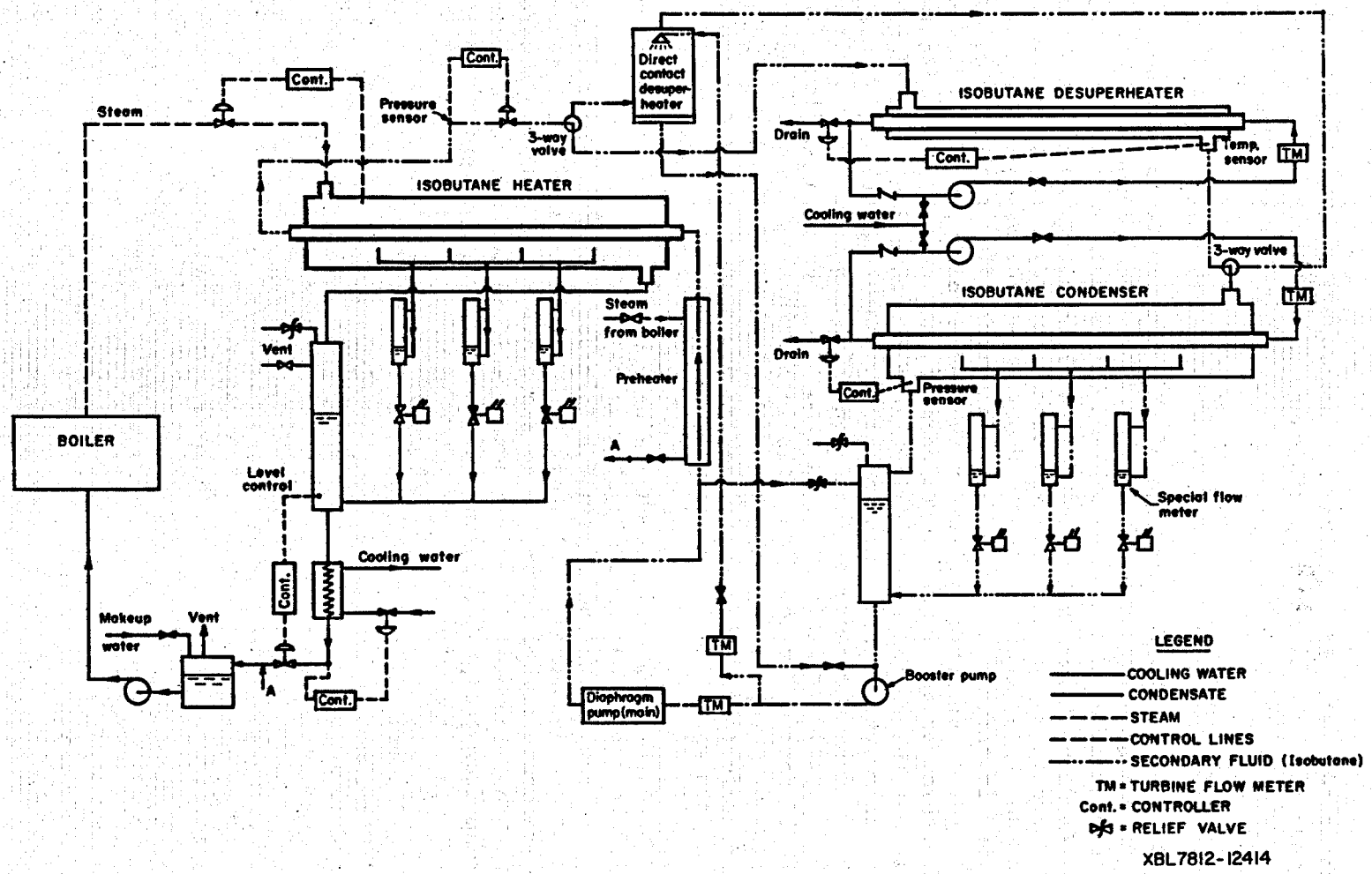

Fig. 8. Detailed flow diagram for the Binary Fluid Experiment.

in the condenser, desuperheater and upstream from the expansion valve was measured by calibrated strain gauge pressure transducers.

Experimental Procedure

Because the basic objective of this program is to provide baseline data to assist designers of binary cycle geothermal power plants in the sizing of heat exchangers, only steady-state data were sought. Data were taken and recorded when conditions in the secondary fluid loop approached steady state. The approach to steady state was excellent in the condenser part of the loop. However, steady state was not as well obtained in the heater at low secondary fluid flow rates due mainly to two factors: pressure cycling in the steam boiler, which caused steam temperature cycling in the steam chest of the heater, and pressure cycling of the secondary fluid in the heater tube due to hunting of the expansion valve. Variation of secondary fluid specific volume is believed to be the cause of expansion valve hunting. The amplitudes of these cyclic variations ranged from 1 percent at high flow rates and to 10 percent at low flow rates in some extreme cases. Increasing the pressure drop through the steam throttling valve and running the boiler at full load help to reduce the variations. Time average values of the data were used in the computations.

The data taken during each run were used to calculate heat balances on different portions of the system as well as calculating the variables needed to compute the heat transfer film coefficient. The bulk temperature of the secondary fluid at different locations inside the heater tube was measured by the traveling probe after all other data were taken so that the flow profile of secondary fluid inside the heater tube, upstream from the probe, was not affected by the movement of the probe.

Initial Results

The apparatus was designed to accept a variety of secondary fluids being considered for use in the binary cycle. Because isobutane has received the most attention, it was decided to start and obtain data on this fluid.

Data were obtained at an average pressure of 4.14 MPa (600 psia) in the heater and at various saturation temperatures and condensate loadings in the condenser. In order to obtain heating data over the range of interest, it was necessary to make runs at various temperatures and flow rates due to the limited size of the instrumented heat transfer surface in the heater.

Figure 9 shows a plot of the inside heat transfer film coefficient, h_i, calculated from Eq. 2, for the heating of isobutane at 4.14 MPa (600 psia) as a function of Reynolds number, Re, where $\dot{m}$ is the weight flow rate of isobutane inside the heater tube, μ is the viscosity of the isobutane at the bulk fluid temperature and D is the inside diameter of the tube. Figure 10 shows a dimensionless plot of these data as a function of Reynolds number where k and c_p represent the thermal conductivity and specific heat of isobutane calculated at the bulk fluid temperature. The solid line shows the Dittus-Boelter correlation with values of transport properties taken from Hanley (1976), and L.F. Silvester, LBL (private communications, 1978) while other properties were taken from thermodynamic tables (ASHRAE, 1969, and Gulf Publishing Company, 1973). The dashed line represents the best fit for the data using the least squares method.

Figure 11 shows a plot of the outside heat transfer film coefficient, h_o, for the condensation of isobutane on the outside of the instrumented tube as a function of the condensate Reynolds number, Re, where Γ represents the condensate rate per unit length of tube and μ_f represents the condensate viscosity. Figure 12 shows a plot of Nusselt number for condensation as a function of twice the condensate Reynolds number where k_f and ν_f represent the thermal conductivity and kinematic viscosity of the isobutane condensate at the vapor temperature and g is the acceleration of gravity. The solid line shows the Nusselt correlation (McAdams, 1954) for isobutane with transport, and thermodynamic properties taken from Hanley (1976), ASHRAE (1969), and Gulf Publishing Company (1973).

There was evidence of some secondary junctions in some of the imbedded thermocouples. These secondary junctions produced erratic thermocouple readings at two stations in the vertical plane. Therefore, the wall temperatures at stations 2 and 4 were used to calculate the average film coefficient for the four-foot long section between stations 2 and 4. The rate of heat input to the isobutane was calculated from the steam condensate collected on the outside of the tube between stations 2 and 4.

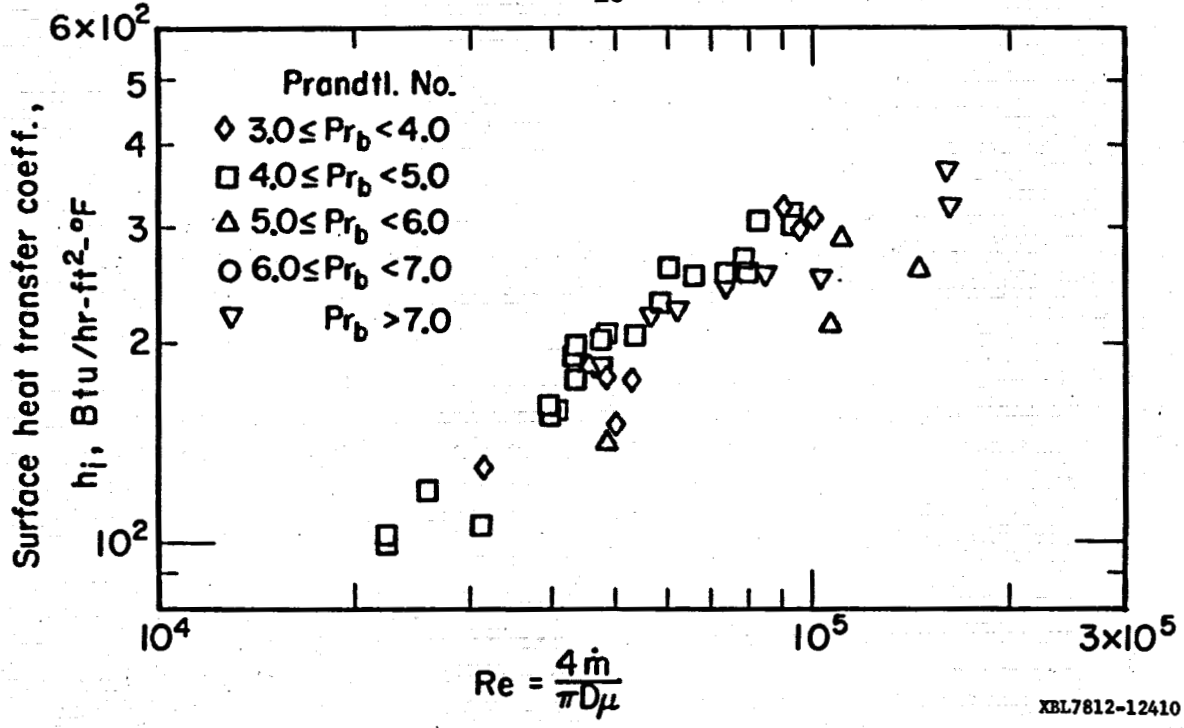

Fig. 9. Film coefficient for heating isobutane inside a tube at 4.14 MPa (600 psia) as a function of Reynolds Number.

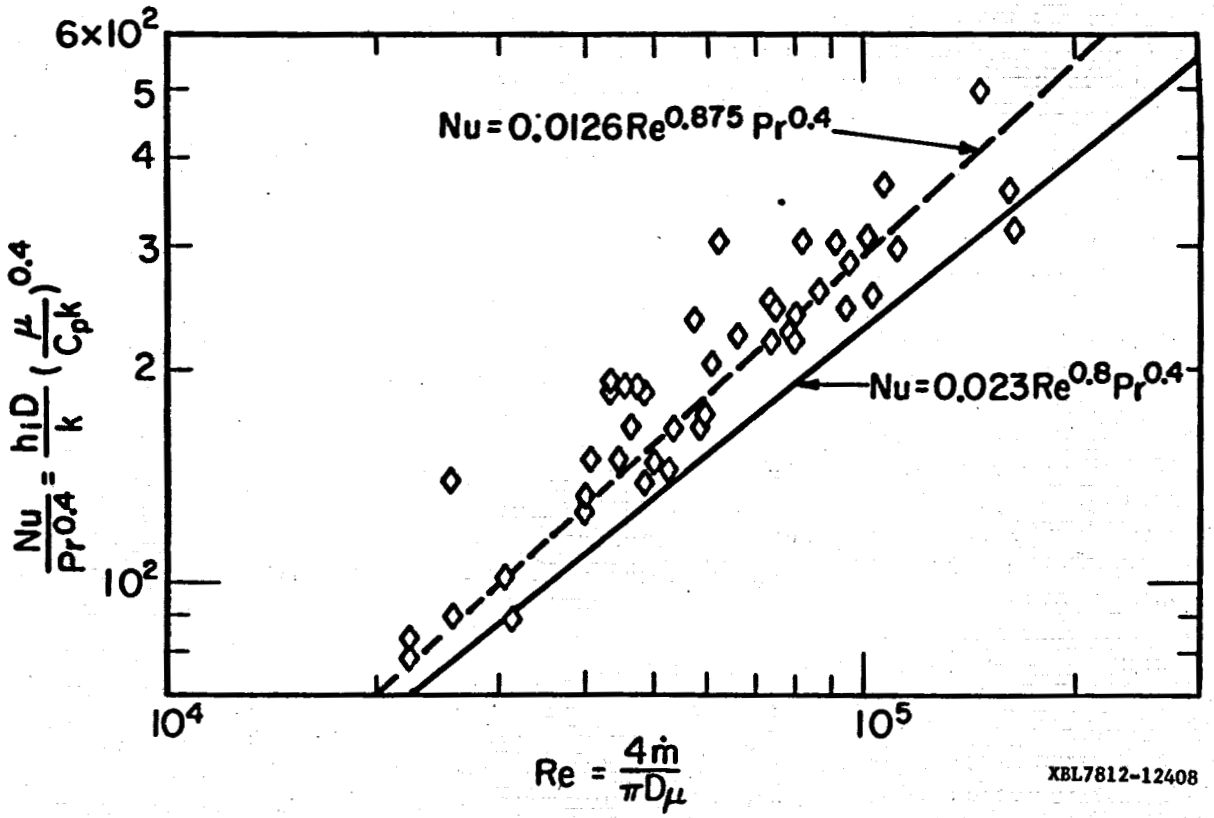

Fig. 10. Dimensionless plot of data on heating isobutane at 4.14 MPa (600 psia). Solid line represents Dittus-Boelter Correlation. Dashed line represents best fit line using least-squares method.

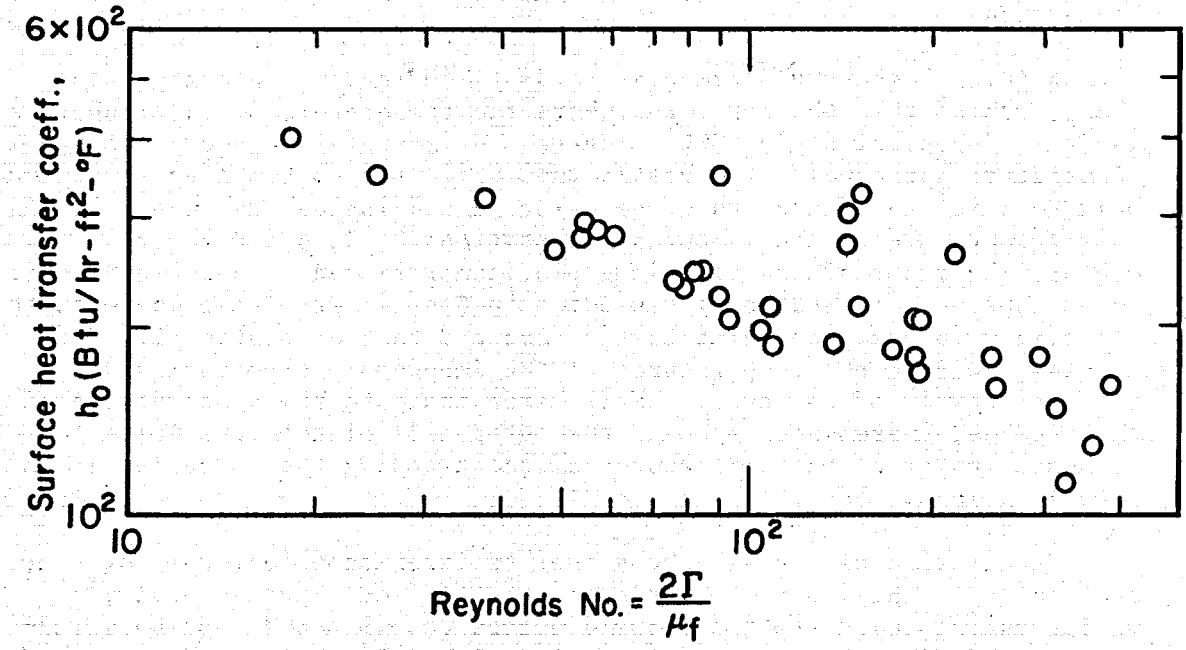

Fig. 11. Film coefficient for isobutane condensing on the outside of a tube as a function of Reynolds Number.

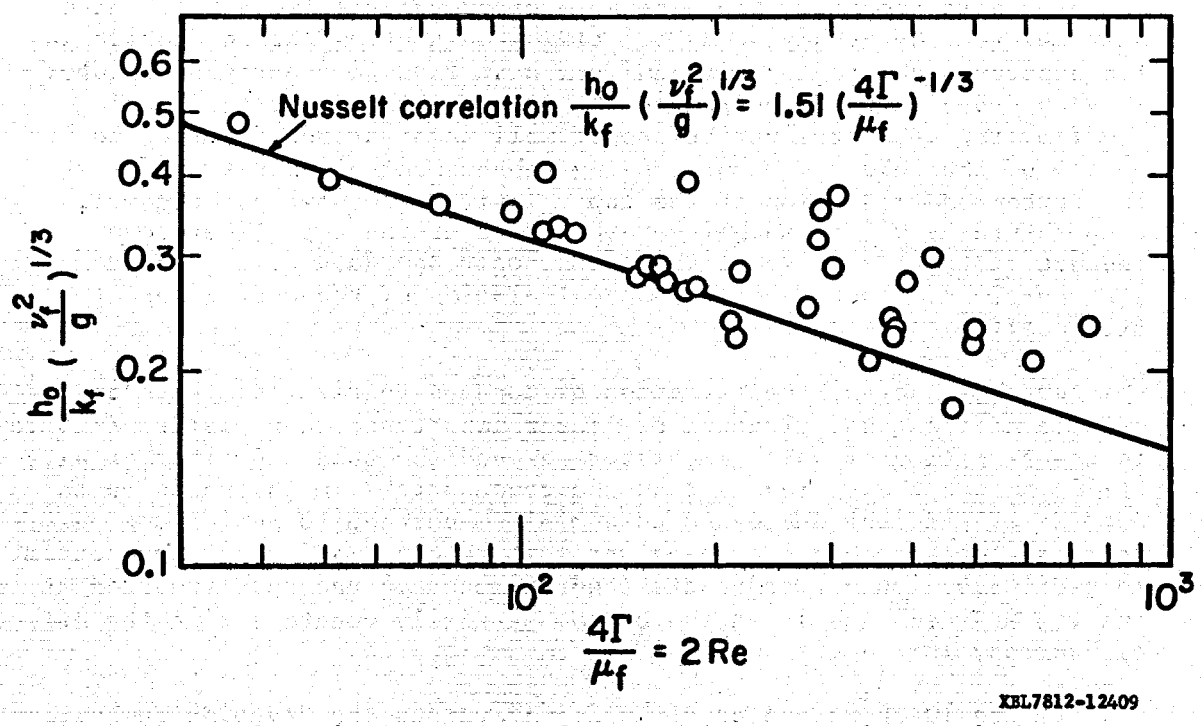

Fig. 12. Dimensionless plot of data on condensation of isobutane on the outside of a tube. Solid line shows the Nusselt Correlation.

Discussion

Figure 13 shows the temperature distribution in the heater along the length of the tube for a run where the temperature of the isobutane was raised approximately 50°C. The top horizontal line shows the steam temperature surrounding the heater tube while the bottom line shows the bulk temperature of the isobutane being heated inside the tube. The bulk temperature of the isobutane at stations 2, 3, 4 and 5 were measured by means of the traveling platinum resistance thermometer while the temperature at station 1 was determined by interpolation between the the temperature at the inlet to the tube and that at station 2. The circles indicate the temperatures of the imbedded thermocouples near the inside wall of the tube. The squares indicate the temperatures of the imbedded thermo-couples near the outer wall of the tube while the diamonds indicate the temperatures of the opposing thermocouples at the same locations.

Examination of Fig. 13 shows that two thermocouples, the outer at station 1 and the inner at station 3, have failed. Consequently, the wall temperature at station 3 could not be determined except by interpolation of temperature between stations 1 and 5. However, because of the shape of the isobutane bulk temperature profile, it was not possible to assume a definite profile for the inner thermocouple temperatures at stations 1, 3, and 5. The two lines connecting stations 1 and 5 and 2 and 4 on Fig. 13 show that the temperature of the inner thermocouples at the top of the tube are higher than those at 90° from the top. This may be due to secondary flows because of buoyancy effects which have been observed by Adebiyi and Hall (1976) on heating carbon dioxide in the supercritical region with uniform heat flux in a horizontal tube. They observed that, depending on the distance from start of heating and flow regime, large variations of wall temperatures from top to bottom of the tube can occur causing enhancement of heat transfer at the bottom and reduction at the top. Their data show that the wall temperature at 90° is much lower than that at the top. Therefore, because of the objective of this work, only the data collected at stations 2 and 4 were used in the calculation of the heat transfer film coefficient.

Another factor, the variation of condensate film thickness on the outside of the tube, although of lesser importance, can also contribute to the variation of wall temperature around the tube. Boelter et al., (1946) showed theoretically that the condensate film thickness on the outside of the tube decreases to a minimum between 10 and 15 degrees from the top and then increases until it reaches maximum at the bottom. This distribution of condensate tends to enhance the heat transfer at the top and decrease it at the bottom partially counteracting the effects of buoyancy inside the tube.

Figure 10 shows a plot of $Nu\ Pr^{-0.4}$ versus the Reynolds number, Re, for the data with transport properties values taken from Hanley (1976) and enthalpy values from thermodynamic tables (ASHRAE,1969, and Gulf Publishing Company, 1973). The solid line shows the Dittus-Boelter

correlation while the dashed line shows the best fit line using the least squares method. It seems that the results of this work show higher values for the inside film coefficient than those predicted from the Dittus-Boelter correlation.

A very important factor in the representation of data is the source for the properties of isobutane because it has a significant effect on the calculation. This is verified on Fig. 14 which shows the values of the thermal conductivity of liquid isobutane as a function of temperature taken from three different sources. The triangles are taken from Natural Gasoline Supply Men's Association (1957), the diamonds were calculated using the API (1970) method while the circles were taken from Hanley (1976). Obviously the choice of the source of properties data will affect the predicted values for the heat transfer film coefficient.

Figure 12 shows a dimensionless plot of the data on condensation of isobutane as a function of condensate loading. The solid line represents the Nusselt prediction for isobutane condensing on the outside of the tube. The data seem to correspond well with the Nusselt correlation up to a Reynolds number of about 100 after which the data produce higher values than those predicted from the Nusselt correlation. This is so because the Nusselt correlation holds only in the laminar regime. The presence of ripples in the condensate film would tend to induce turbulence and lower the average film thickness resulting in enhancement of heat transfer. Kapitsa (Kutateldaze, 1963) has predicted that ripples in the condensate film can begin to form at a Reynolds as low as 5 for propane.

The isobutane turbine flowmeter readings were not used because of fluctuating readings caused by cyclic variation of suction pressure at the inlet to the high pressure pump. Consequently, for all of these runs, the mass flow rate of the isobutane inside the heater tube was calculated from a heat balance on the heater tube between stations 2 and 4. Therefore, since no direct measurement of isobutane flow rate was available, the results presented in this report on the heater are considered by the authors to be preliminary. However, since the condensation rate of isobutane in the condenser was measured directly by the special flow meters, and as the effects of buoyancy on the cooling water inside the tube are negligible due to its high flow rate, and as the results on condensation were repeatable, it is believed that the results presented on Figs. 11 and 12 can be used with confidence over the range shown.

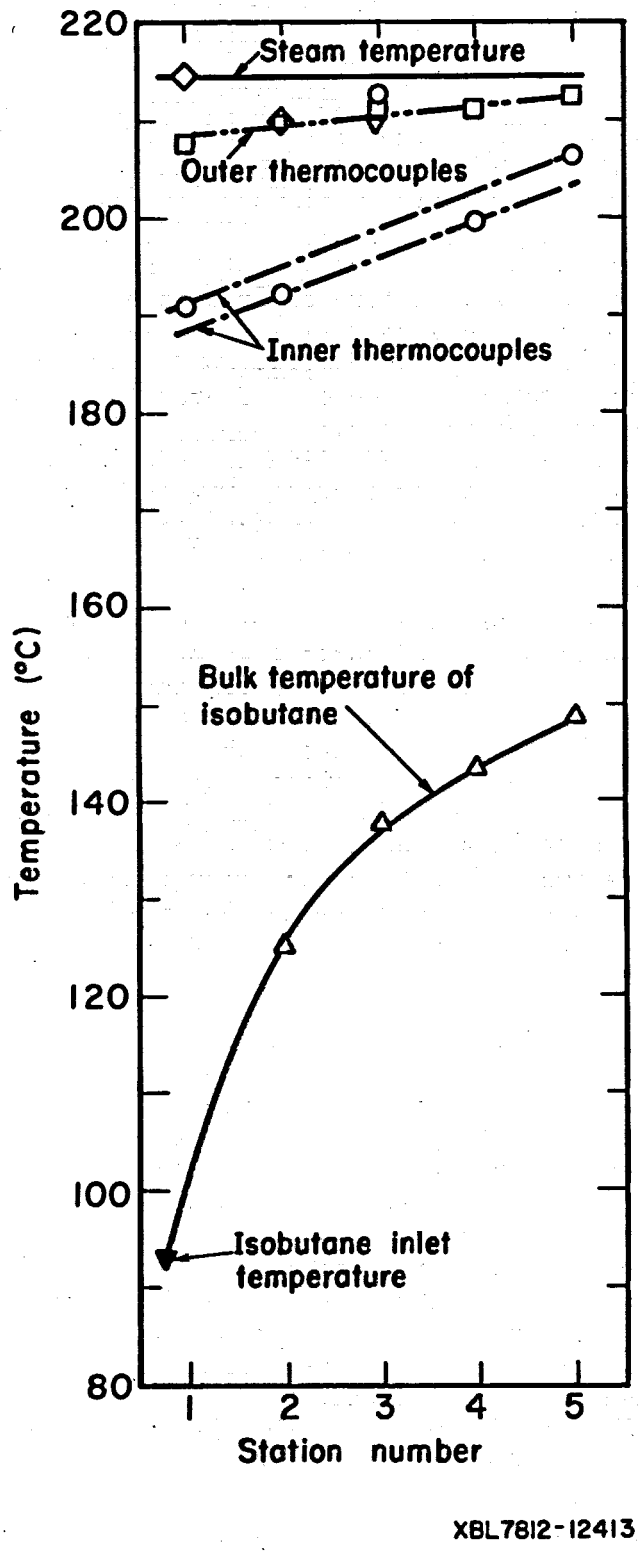

Fig. 13. Temperature profile along the heater for Run 118.

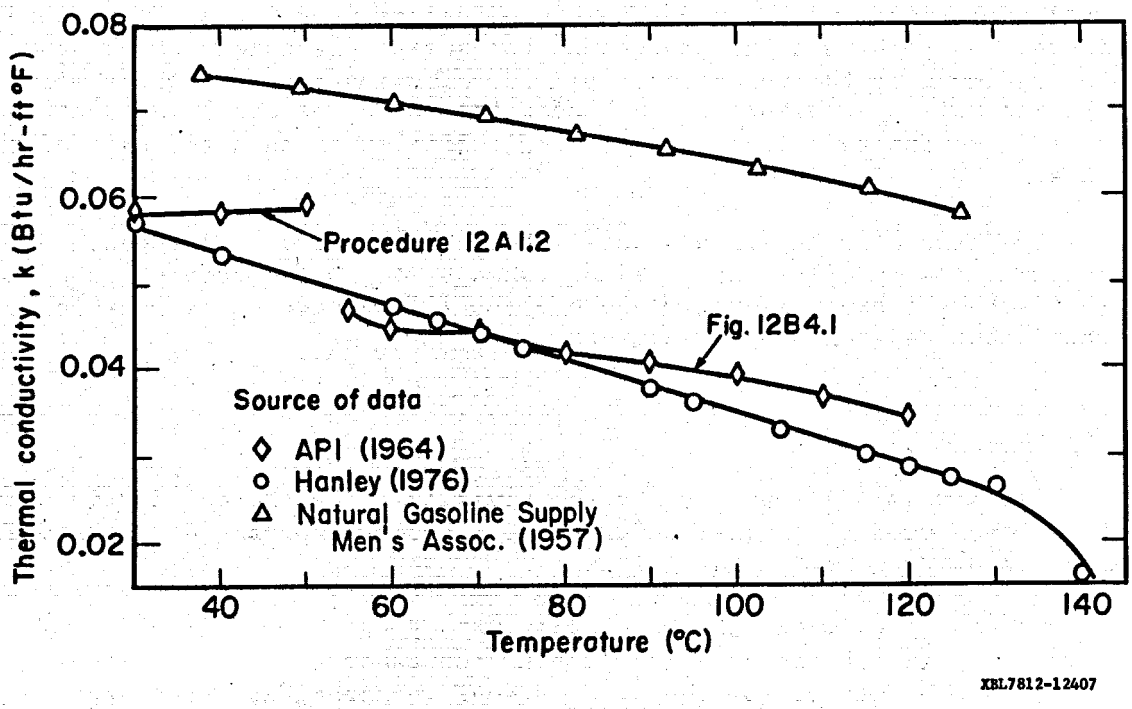

Fig. 14. Thermal conductivity of saturated liquid isobutane as a function of temperature. Points are plotted from three references.

Future Plans

Since the preliminary data presented in this report were taken, noncondensable gas accumulation in the heater chest has been eliminated by adequate venting and the turbine meter to measure the isobutane flow rate was moved downstream of the high pressure pump. Also, the instrumented tubes in both the heater and condenser were taken out and the faulty imbedded thermocouples repaired. The instrumented tubes were then installed such that the imbedded thermocouples are located at 45° above a horizontal plane passing longitudinally through the axis of the tube.

Additional data for heating isobutane at various pressures, temperatures and flow rate will be taken next. After completion of the isobutane experiments, measurements will be made on isopentane and isobutane/isopentane mixtures.

Acknowledgment

This work was supported by the Division of Geothermal Energy of the U.S. Department of Energy, under contract No. W-7405-ENG-48, with Clifton McFarland, Program Manager.

The authors wish to acknowledge the support and cooperation of the personnel at both the Sea Water Conversion Laboratory and Lawrence Berkeley Laboratory. Of the many persons who provided assistance in the design, construction and assembly of the experiment, the following persons deserve special mention: C. Adair Roberts, Milton C. Moebus, Donald R. Lippert, Donald R. Bliss, Winston E. Canady, Eugene P. Binnall and Richard E. Whiteman of the Lawrence Berkeley Laboratory; Justin C. Hensley and Galen P. Schwab of the Sea Water Conversion Laboratory; John Cole of the Richmond Field Station Machine Shop; and last, but not least, thanks and appreciation to Kenneth F. Mirk and Robert L. Fulton of LBL for their cooperation, encouragement and readiness to lend a needed hand.

References Cited

Adebiyi, G.A. and Hall, W.B., 1976. Experimental investigation of heat transfer to supercritical pressure carbon dioxide in a horizontal pipe. Inter. Jour. Heat Mass Transfer, v. 19, pp. 715-720.

American Petroleum Institute, 1970. Technical data book-Petroleum refining. Second ed., Chapter 2, pp.5-23.

American Society of Heating, Refrigerating, and Air-Conditioning Engineers, 1969. ASHRAE thermodynamic properties of refrigerants.

Boelter, L.M.K. et al., 1946. Heat transfer notes. Berkeley: University of California Press, Chapter XV.

Green, M.A. and Pines, H.S., 1975. Calculations of geothermal power plant using Program GEOTHM. Proceedings of Second United Nations Symposium on the Development and Use of Geothermal Resources, San Francisco, May 1975, v. 3, p. 1965. (Also, Lawrence Berkeley Laboratory report, LBL-3238.)

Gulf Publishing Co., 1973. Fluid thermodynamic properties of light hydrocarbons. Houston: Gulf Publishing Co.

Hanley, H.J.M., 1976. Prediction of the viscosity and thermal conductivity coefficients of mixtures. Cryogenics, Nov. 1976, pp. 643-652.

Kutateladze, S.S., 1963. Fundamentals of heat transfer. Arnold Publishing Co., English translation, pp. 307-308.

McAdams, W.H., 1954. Heat transmission. Third ed., New York: McGraw-Hill, p. 338.

Natural Gasoline Supply Men's Assoc., 1957. Engineering data book.

Roberts, V.W., 1976. Geothermal energy conversion and economics--case studies. Palo Alto: Electric Power Research Institute. EPRI ER-301, Project 580, Topical Report 2, Nov. 1976.

Rogers Engineering Co., Inc. and Benham-Blair and Affiliates, 1974. 10 MW experimental geothermal power plant conceptual design: pre-title 1 report. San Francisco: prepared for U.S. AEC/ Lawrence Berkeley Laboratory, Sept. 1974.

Wollenberg, H.A. et al., 1975. Geothermal resource assessment. Lawrence Berkeley Laboratory, Report UCID-3762.

U.S.GPO:1979-689-058/(F)8